SCIENTIFIC AND TECHNICAL SECTION

UDC 539.4

FEM Analysis and Experimental Study on the Bending Strength of Ceramic Tiles with the Top- and Back-Sided Polyurea Coating

K. Kamonchaivanich,[1] K. Kuboyama, and T. Ougizawa

Department of Chemistry and Materials Science, Tokyo Institute of Technology, Tokyo, Japan

[1] kamonchaivanich.k.aa@m.titech.ac.jp

Mechanical properties enhancement of ceramic tiles by a simple coating technique using polyurea was investigated. Solventless polyurea coatings were employed. The effect of coating sides of the ceramic substrate and film thickness on the mechanical properties were examined in three-point bend tests. The back-coated ceramic tile demonstrated a significant improvement in bending strength (by 25–50%) as compared to the top-coated one. The stress distribution in the substrate was analyzed by the finite element method, and the mechanism of improving mechanical properties was discussed. Based on FEM analysis, the polyurea back-coating appeared to be more effective as regards the stress distribution. The stress distribution in the back-coated ceramic tile is more uniform due to the cushioning effect of the supporting pins. The mechanism of the polyurea coating effect was evaluated in the experiment and finite element analysis. It was established that the stress distribution due to the polyurea coating was of importance for the improvement of the bending strength of substrates.

Keywords: polyurea, coating, ceramic tile, bending strength, stress distribution, finite element analysis.

Introduction. Polyurea is widely used as the protective materials for various applications, such as the building, flooring, bridges and armor because of its excellent mechanical performance and elastomeric property [1]. As shown in Fig. 1, polyurea is derived from the reaction of an isocyanate with an amine, resulting in the urea formation. It can be treated as 100% solid, catalyst-free, and environmental-friendly material [2].

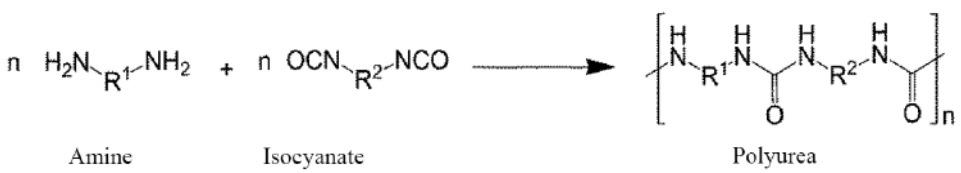

Fig. 1. Polyurea formation from isocyanate and amine (R^1 and R^2 = alkyl or aryl groups).

Recently, polyaspartic ester based polyurea which is a new generation of two-component aliphatic polyurea containing isocyanate components; trimers or dimers of hexamethylene diisocyanate, has been developed. A coating of elastomeric polyurea on various substrates as the protective materials has been widely studied. In impact resistance study, samples of concretes were sprayed with polyurea and a drop test of coated concretes from a height of 1.8 m was performed. The concrete cracked, but the polyurea coating was

undamaged and supported the concrete debris [3]. Rijensky and Rittel [4] studied the importance of the coated side of the polyurea with a response of water-shocked polyurea coated aluminum plates. The polyurea layer enhances the overall rigidity of the layered plate and also reduces deflections. No signs of erosion in the center if the side of the coating was positioned on the wet side of the plate. Besides the concrete substrates, a polyurea coating on steel plates was also examined by Ackland et al. [5]. Steel plates with and without polyurea coating applied to back surface were compared. Numerical investigations were lead to assess the effect of coating thickness and coating location (front, back or sandwich between two plates) on deformation, both experimentally and numerically using ANSYS software. The sandwich plate and top coating did not show any improvement over uncoated steel plate, compared with 5 mm plate with back face coating. In addition, the plates with polyurea coatings resulted in higher plate deformation, increasing with coating thickness. Gardner et al. [6] reported the effect of a position of polyurea sheet inserted between a sandwich composite. A blast mitigation of this composite material was investigated by using a shock tube apparatus. The sandwich composite consisted of top and back facesheets poly(vinyl ester) and foam core poly(styrene-co-acrylonitrile). The polyurea sheet was inserted either before or behind the foam core. It was found that inserting the polyurea behind the foam core was more effective in terms of energy absorption. The deformation energy was reduced by 25%. Thus the overall blast performance was improved while the structural integrity was maintained. Wang et al. [7] reported an application of polyurea to reinforce a clay brick masonry wall. The study shows that polyurea can partially reinforce the brick wall. Moreover, the coating at thickness of 3 mm increased the blast resistance by more than 4 times, compared to unreinforced wall. Polyurea has exhibited the high potential for enhancing the mechanical properties of building materials. However, mechanism of enhancements has not been investigated clearly.

In this study, we therefore aimed to improve the mechanical property of ceramic tile as a building material by using polyurea coating, and reduce a risk of injury from sharply-cracked debris during disasters, such as earthquake. The elastomeric polyurea coating is expected to firmly support the cracked debris, even if it is completely cracked. In many studies, polyurea shows a high performance for improving the mechanical properties and durability. However, mechanism of improvement is still not completely verified. The aim of this study is to investigate the critical factors which enhance the flexural strength by polyurea coating and clarify the mechanism. Effects of coating sides and thickness of coating on substrate were investigated.

1. **Experimental**. The earthenware ceramic floor tile was used as a substrate. This ceramic tile was produced by COTTO, Co., Ltd., Thailand. Water absorption is approx. 5–8%, due to highly porous ceramic. Aspartic acid ester (Desmophen®NH2850XP) was used as the polyurea precursor. Aliphatic polyisocyanate based on hexamethylene diisocyanate (HDI), (Desmodur®N3900) was used as the resin hardener. All chemicals were supplied by Covestro (Germany). Properties of aspartic acid ester and aliphatic polyisocyanate are shown in Table 1. To form the polyurea (PU) coating, the aspartic acid ester was mixed with the aliphatic polyisocyanate at weight ratio of 1.6 and cured at room temperature for 7 days before testing. The elastic modulus and strain at break of polyurea was estimated from tensile test as 240 MPa and 280%, respectively.

T a b l e 1

Properties of Aspartic Acid Ester and Aliphatic Polyisocyanate Used in This Study

Materials	Commercial name	Amine value (mg KOH/g)	%NCO	Viscosity (mPa · s)
Aspartic acid ester	Desmophen®NH2850XP	190	–	100
Aliphatic polyisocyanate	Desmodur®N3900	–	23.0–24.0	630–830

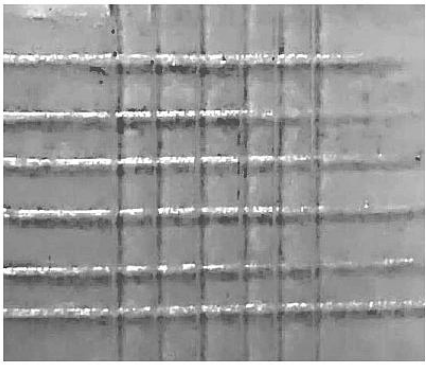

Fig. 2. Adhesion test result of polyurea film on the ceramic substrate after pulling tape test.

The adhesion test of the polyurea coating to the ceramic substrate was performed in accordance with ASTM Test Method D3359 (cross-cut), and the adhesion of the polyurea on the ceramic used in this study was classification 5B (edges of cuts completely smooth) as shown in Fig. 2.

1.1. ***Sample Preparation***. A mixture of aspartic acid ester and HDI was used to form the polyurea coating. The mixture was immediately applied either on the top or the back side of the substrates by using applicator bar as presented in Fig. 3. The coating thickness was varied from 200, 300, 400, 500, 800, and 1000 μm. Coating thickness is in a range of 200–400 μm, and 500–1000 μm with the deviation of ± 10 and $\pm 6\%$, respectively. The thickness was measured by a micrometer. The fractured surface after three-point bending test was observed by scanning electron microscopy (SEM; SM-200, Topcon Corp., Japan). The sample was cut to a dimension of 15×100 mm with thickness of 6 mm.

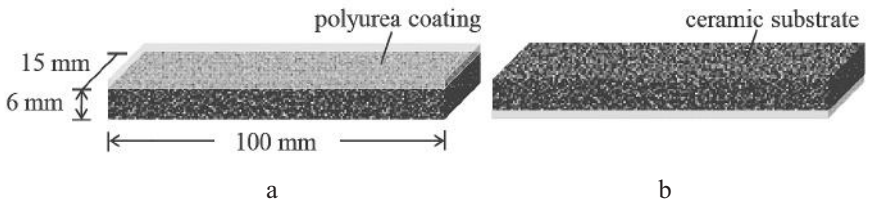

Fig. 3. Schematic of polyurea coating sides on the ceramic substrates: (a) top coat and (b) back coat.

1.2. ***Three-Point Bending Test***. Three-point bending test was carried out by using a universal material testing instrument (Tensilon RTC-1350A, A&D) with a span of 40 mm at a crosshead speed of 1 mm/min. For a rectangular sample under a load in a three-point bending, the flexural strength was measured using the following Eq. (1) [8]:

$$\text{Flexural strength} = \frac{3FL}{2bd^2}, \tag{1}$$

where F is the load at the fracture point, L is the length of the support span, b is the width, and d is the total thickness of substrate and coating.

1.3. ***Simulation by Finite Element Method (FEM)***. A simulation of stress concentration in the specimen during the three-point bending test was performed by finite element method using ABAQUS^{TM} software (Dassault Systemes Simulia Corp.). Considering the 3D model results, stress concentration are compared between uncoated substrates, and top/back coated ones. Thickness of coating and ceramic substrate was 1000 μm and 6.0 mm, respectively.

The mesh sizes of ceramic substrate and film are 1.0 mm. The total number of elements and nodes were 10,500 and 12,928, respectively. The delamination and breakage of specimen were not considered in this model. Table 2 shows the input parameters of materials for FEM simulation. The elastic modulus (E) of ceramic substrate was determined from the following Eq. (2) [9]:

$$E = \frac{L^3 A}{4bd^3}, \tag{2}$$

where L is the span length, A is the slope of the load–displacement curve of bending test in the linear region, and b and d are the sample width and thickness, respectively.

T a b l e 2

Material Properties Used in Finite Element Method

Materials	Elastic modulus (MPa)	Poisson's ratio
Earthenware Ceramic	4515	0.25 [10]
Polyurea	240	0.33 [11, 12]

2. **Results and Discussion**.

2.1. ***Effects of Coating Sides and Coating Thickness on the Flexural Strength of Ceramic Tile***. The load–displacement curves of uncoated, top-coated and back-coated ceramic substrates measured by three point bending test were obtained as shown in Fig. 4. The coating thickness was 500 μm. All samples fractured in a brittle manner. The displacements at break of the coated substrates were larger than the uncoated one. This result suggests that the deformation of coating films played important role for their difference, that is, the deformation occurred in the top-coated ceramic where the load was applied and in the back-coated one where the two supporting pins contacted. When the coated substrates are compared each other, the back-coated ceramic showed higher load at break than the top-coated one. To analyze the coating effect on the mechanical property, the flexural strength of the samples with the top coat and the back coat was evaluated at different coating thickness as shown in Fig. 5.

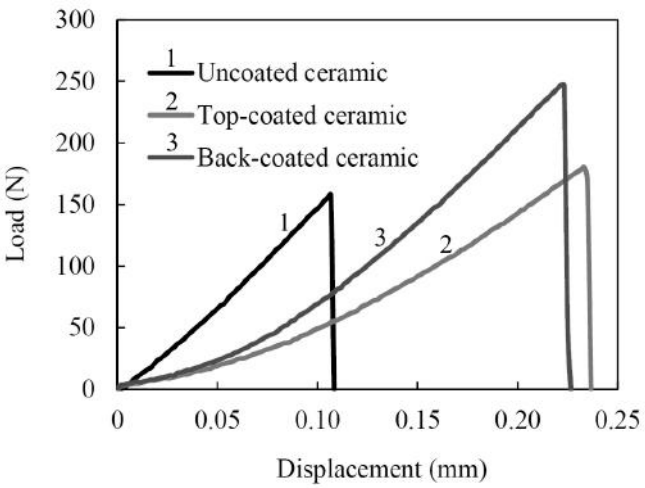

Fig. 4. Load–displacement curves of uncoated, top- and back-coated ceramic. (Coating thickness of 500 μm.)

Figure 5 shows the flexural strength of the samples with the top coat and the back coat at different coating thickness. Flexural strength was calculated by total thickness of substrate and coating. However, we found whether the film thickness is included or excluded in the calculation, the results clearly show that the back-coated ceramic has higher flexural strength than top-coated one. Moreover, it was found that the back-coated ceramic exhibited the higher flexural strength than the top-coated ceramic in any thicknesses used in this study, while no significant improvement of the flexural strength was observed by the top-coated ceramic. The flexural strength of the substrate was improved by increasing of back coating film with thickness up to about 500 μm. More importantly, the thicker coating of 800 and 1000 μm showed the steep drop of flexural strength. In such samples, delamination at the interface between the polyurea coating film and the ceramic tile was observed.

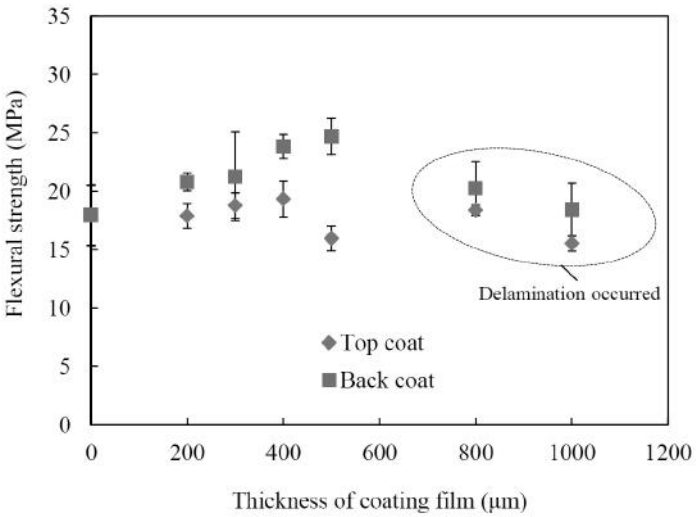

Fig. 5. Effects of coating sides on the flexural strength of ceramic tile analyzed by three-point bending test.

Figure 6 demonstrates the SEM micrographs of fracture surface of the back-coated ceramic substrate with the 1000 μm thick polyurea coating after three-point bending test. In this micrograph, delamination was clearly observed. The delamination was also observed in the samples with the coating thicker than 500 μm, but it was not observed in the samples with less than 500 μm. The delamination in the samples with thicker coating implies that the internal stress generated during the three point-bending test became larger than the adhesion strength because of plane strain condition [13, 14] in the thicker coating films. Moreover, the delamination must be the reason why the flexural strength was not improved in the samples with the coating thicker than 500 μm.

2.2. ***Analysis of Effects of Coating Sides by FEM***. To reveal the reason why the flexural strength of substrate depended on coating sides (top coat and back coat), the simulation using FEM was carried out. The ceramic substrate with the coating of 1000 μm thickness was analyzed in this study because it is expected that thicker film is more effective for improvement of the flexural strength, if the delamination does not take place. Fig. 7a–c show the simulation results of uncoated, top-coated and back-coated ceramic substrates, respectively. It is known that maximum principal stress is normally valid for brittle materials, and then the FEM results were shown by contour plots of maximum principal stress [15, 16]. In this plot, the negative value of maximum principal stress means that the component is in compression and positive in tension [17]. From the plots, it was obvious that the tensile stress concentration occurs around the center bottom of the

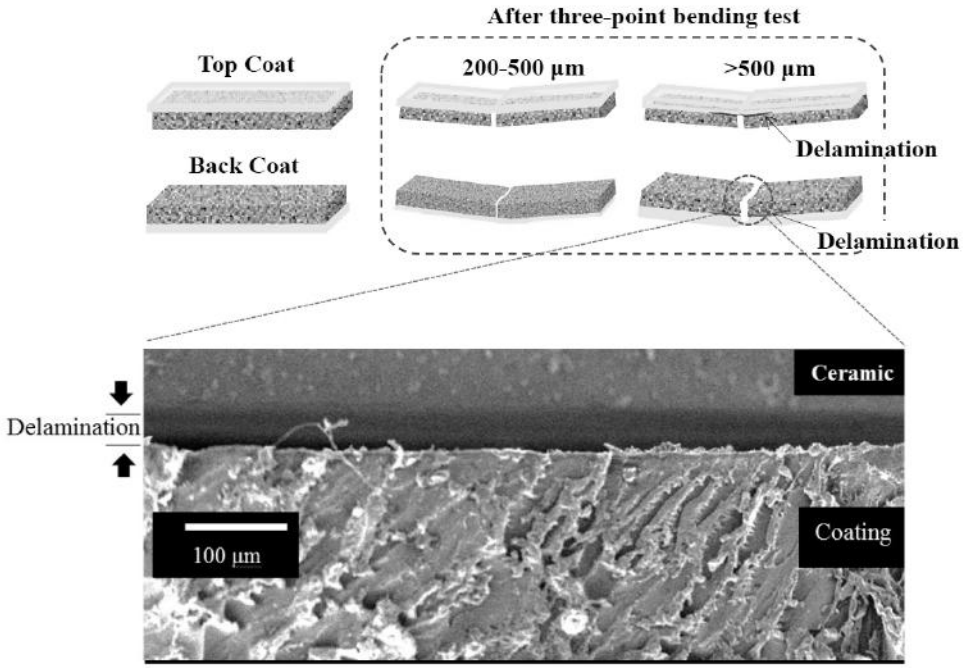

Fig. 6. SEM micrographs of fracture surface of back-coated ceramic substrate after three-point bending test with coating thickness of 1000 μm.

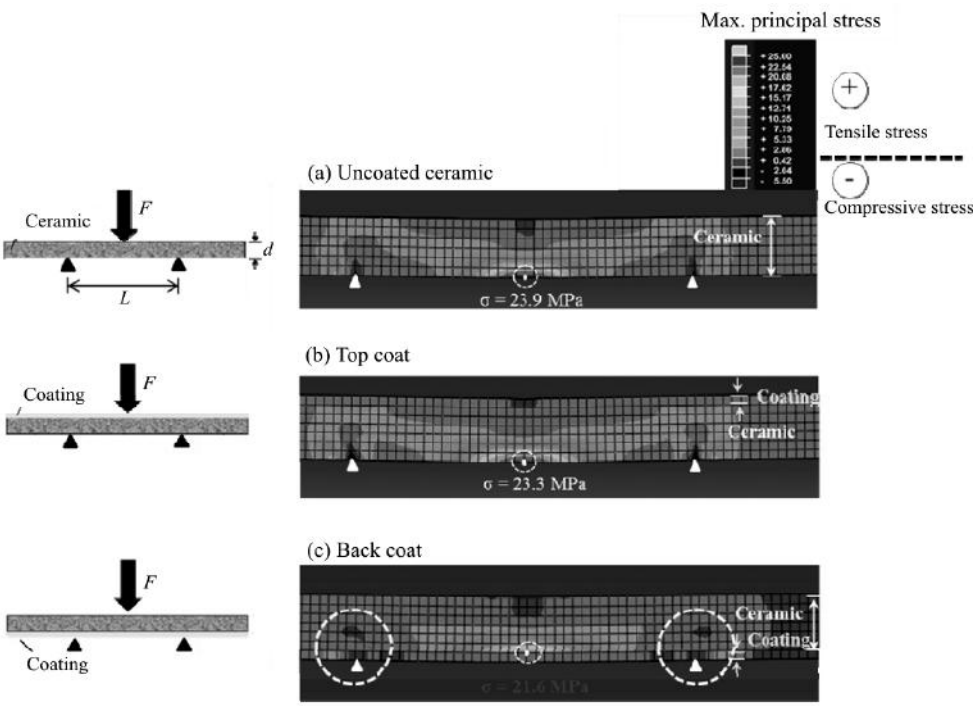

Fig. 7. FEM simulation of three-point bending of side view contour plot of maximum principal stress of (a) uncoated ceramic, (b) top-coated ceramic, and (c) back-coated ceramic at the displacement of 0.3 mm and coating thickness of 1000 μm.

substrate in all samples, while the compressive stress concentration does around the top center and bottom support medium in the three point bending test. In case of bending test of brittle material such as ceramics, glass etc., it is known that compressive stress concentration occurs at the top center and tensile stress concentration does at the bottom center, and fracture starts around the point where the maximum tensile stress concentration occurs [18, 19]. Therefore, the tensile stress concentration at the bottom of specimen was considered to be a crucial factor in the cracking of brittle samples used in this study.

From Fig. 7a and b, the maximum tensile stresses at the bottom center of uncoated and top-coated ceramic were 23.9 and 23.3 MPa, respectively (at the displacement 0.3 mm), whereas that of interface of back-coated ceramic substrate (Fig. 7c) was 21.6 MPa (9.6 and 7.3% decreased from the uncoated and top-coated ceramic, respectively). Moreover, back-coated ceramic showed that the compressive stress at interface between bottom of ceramic substrate and coating around the supporting pins was also lower than the others.

Figure 8 shows the results of the maximum principal stress along the bottom of ceramic substrate by distance from the center by FEM simulation of three-point bending. Considering the range from +1.5 to +2.5 cm and −1.5 to −2.5 cm from center of substrate, the results show that the compressive stress distribution at the interface between back-coated ceramic and coating was the lowest. At the supporting pins (±2.0 cm), stress of back-coated interface was nearby −1 MPa whereas tensile stresses of top-coated ceramic and uncoated ceramic were the same at −3 MPa. In addition, at position ±2.2 cm at outer position of supporting pins, tensile stresses of top-coated and uncoated samples was around 12 and 17 MPa, respectively, but stress of back-coated interface was nearby 0 MPa. This result could be called “cushion effect”. In the back-coated ceramic, the tensile stress distribution between −1.8 and +1.8 cm was broader than those of the others, and it implies that the cushion effect contributes such the stress distribution. Because of the stress dissipation, the tensile stress concentration at the center bottom of back-coated ceramic was reduced.

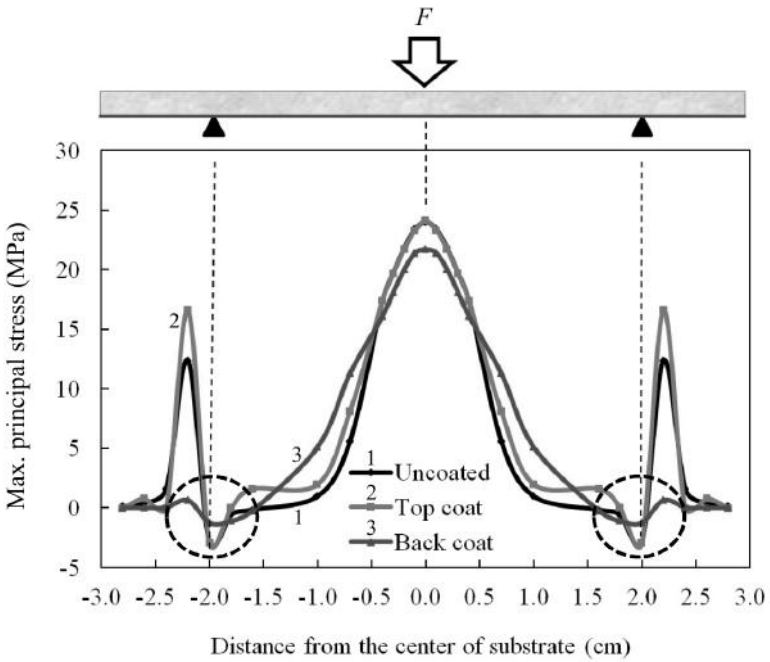

Fig. 8. FEM simulation of three-point bending of stress distribution at bottom of uncoated ceramic, top-coated ceramic and back-coated ceramic at the displacement of 0.3 mm and coating thickness of 1000 μm.

Conclusions. The effects of polyurea coating to ceramic tile on the mechanical properties were investigated experimentally by the three point bending test and numerically analyzed by FEM simulation. The effects of coating sides and coating thickness were examined. As the result, it was found that the back-coated polyurea on the ceramic substrate improved the flexural strength of the substrate, while the top-coated one showed no effect. Thicker coating film improved the strength more, however, the delamination of the coating from the substrate was also observed in the thicker coating samples and it resulted in the lowering of the improvement of the flexural strength. In this study, the mechanism of effect of coating side demonstrated in stress distribution of ceramic substrate and coating film. Moreover, the finite element method revealed that the mechanism of the improvement of flexural strength by the back coating was due to the cushion effect and the reduction of tensile stress around the bottom center of substrate.

1. K.-F. Torges and D. J. Primeaux II, "Cast polyurea elastomers, application, processing and performance," in: UTECH'94, Paper 42, Netherlands Congress Center, Den Hague (1994), pp. 1–8.
2. D. J. Primeaux II, *Polyurea Elastomer Technology: History, Chemistry & Basic Formulating Techniques*, Primeaux Associates LLC, Texas (2004).
3. A. A. Tracton, *Coating Technology Handbook*, Third edition, CRC Press, New York, (2005).
4. O. Rijensky and D. Rittel, "Polyurea coated aluminum plates under hydrodynamic loading: Does side matter?" *Int. J. Impact Eng.*, **98**, 1–12 (2016).
5. K. Ackland, C. Anderson, and T. D. Ngo, "Deformation of polyurea-coated steel plates under localised blast loading," *Int. J. Impact Eng.*, **51**, 13–22 (2013).
6. N. Gardner, E. Wang, P. Kumar, and A. Shukla, "Blast mitigation in a sandwich composite using graded core and polyurea interlayer," *Exp. Mech.*, **52**, 119–133 (2012).
7. J. G. Wang, H. Q. Ren, X. Y. Wu, and C. L. Cai, "Effect of polyurea reinforced masonry walls for blast loads," in: Advances in Energy, Environment and Materials Science: Proc. of the 2nd Int. Conf. on *Energy, Environment and Materials Science* (EEMS 2016, July 29–31, 2016, Singapore), CRC Press, New York (2016), pp. 331–338.
8. *ASTM C1161-13. Standard Test Method for Flexural Strength of Advanced Ceramics at Ambient Temperature*, ASTM International, West Conshohocken, PA (2013).
9. F. Hafeez and M. Arif, *Engineering Practical Book Vol-II: Basic Mechanics and Science of Materials*, eBooks2go Inc. (2011).
10. R. W. Davidge, *Mechanical Behaviour of Ceramics*, Cambridge, New York (1979).
11. G. N. Greaves, A. L. Greer, R. S. Lakes, and T. Rouxel, "Poisson's ratio and modern materials," *Nat. Mater.*, **10**, 823–837 (2011).
12. V. Orlov, "Computer simulation of optimal thickness of polyurea coating using for trenchless renovation of potable water pipes," *Procedia Engineer.*, **165**, 1168–1175 (2016).
13. http://www.digitaleng.news/de/simplifying-fea-models-plane-stress-and-plane-strain/
14. E. C. Teixeira, J. R. Piascik, B. R. Stoner, and J. Y. Thompson, "Effect of YSZ thin film coating thickness on the strength of a ceramic substrate," *J. Biomed. Mater. Res.*, **83B**, 459–463 (2007).
15. D. Gross and T. Seelig, *Fracture Mechanics: With an Introduction to Micromechanics*, Chapter 2, Springer, Berlin (2011).

16. I. N. Koukoulis, C. G. Provatidis, and S. Georgiou, “Finite element modelling of the mechanical effects of the UV laser ablation of polymer coatings,” *J. Appl. Surf. Sci.*, **254**, 3531–3539 (2008).
17. A. Ahmad, *Handbook of Optomechanical Engineering*, CRC Press, New York (1996).
18. R. L. Norton, *Machine Design: An Integrated Approach*, Pearson Prentice Hall, New York (1996).
19. S. W. Freiman and J. J. Mecholsky, Jr., *The Fracture of Brittle Materials Testing and Analysis*, John Willy & Sons, New Jersey (2012).

Received 05. 03. 2018